

## Effects of autotaxin and lysophosphatidic acid deficiencies on depression-like behaviors in mice exposed to chronic unpredictable mild stress

Chao Wang<sup>a,c,1</sup>, Ningyuan Li<sup>a,1</sup>, Yuqi Feng<sup>a</sup>, Siqi Sun<sup>a</sup>, Jingtong Rong<sup>a</sup>, Xin-hui Xie<sup>a</sup>, Shuxian Xu<sup>a</sup>, Zhongchun Liu<sup>a,b,\*</sup>

<sup>a</sup> Department of Psychiatry, Renmin Hospital of Wuhan University, Wuhan, Hubei, PR China

<sup>b</sup> Taikang Center for Life and Medical Sciences, Wuhan University, Wuhan, PR China

<sup>c</sup> Department of Neurology, Wuhan Fourth Hospital, Wuhan, Hubei, PR China

### ARTICLE INFO

#### Keywords:

Depression  
Lipid  
Autotaxin  
Lysophosphatidic acid  
Synapse

### ABSTRACT

The involvement of lipids in the mechanism of depression has triggered extensive discussions. Earlier studies have identified diminished levels of lysophosphatidic acid (LPA) and autotaxin (ATX) in individuals experiencing depression. However, the exact significance of this phenomenon in relation to depression remains inconclusive. This study seeks to explore the deeper implications of these observations. We assessed alterations in ATX and LPA in both the control group and the chronic unpredictable mild stress (CUMS) model group. Additionally, the impact of ATX adeno-associated virus (AAV-ATX) injection into the hippocampus was validated through behavioral tests in CUMS-exposed mice. Furthermore, we probed the effects of LPA on synapse-associated proteins both in HT22 cells and within the mouse hippocampus. The mechanisms underpinning the LPA-triggered shifts in protein expression were further scrutinized. Hippocampal tissues were augmented with ATX to assess its potential to alleviate depression-like behavior by modulating synaptic-related proteins. Our findings suggest that the decrement in ATX and LPA levels alters the expression of proteins associated with synaptic plasticity *in vitro* and *in vivo*, such as synapsin-I (SYN), synaptophysin (SYP), and brain-derived neurotrophic factor (BDNF). Moreover, we discerned a role for the ERK/CREB signaling pathway in mediating the effects of ATX and LPA. Importantly, strategic supplementation of ATX effectively mitigated depression-like behaviors. This study indicates that the ATX-LPA pathway may influence depression-like behaviors by modulating synaptic plasticity in the brains of CUMS-exposed mice. These insights augment our understanding of depression's potential pathogenic mechanism in the context of lipid metabolism and propose promising therapeutic strategies for ameliorating the disease.

### 1. Introduction

Major depressive disorder (MDD) is one of the most prevalent mental disorders, impacting approximately 350 million individuals worldwide. Even with therapeutic interventions, a notable portion of patients fail to achieve a satisfactory response to treatment (Gaynes, 2016). The pathogenesis of depression has long been enigmatic, and understanding the intricate mechanisms that underlie depression is essential for addressing its onset and progression. In recent years, an increasing body of evidence

has highlighted the significant potential of lysophosphatidic acid (LPA) molecules in elucidating this complexity (Kim et al., 2018).

While most lipid-related depression studies predominantly rely on plasma samples, it is crucial to consider that depression is a brain disorder. Assessing lipid indicators in peripheral blood, primarily influenced by peripheral status, may only offer an indirect reflection of the central nervous system (CNS) status. Two studies utilizing cerebrospinal fluid (CSF) have provided valuable insights, revealing a significant decrease in both LPA and autotaxin (ATX, ENPP2), an enzyme crucial for

\* Corresponding author. Department of Psychiatry, Renmin Hospital of Wuhan University, No. 99 Jiefang Road, Wuchang District, Wuhan, Hubei, 430060, PR China.

E-mail address: [zcliu6@whu.edu.cn](mailto:zcliu6@whu.edu.cn) (Z. Liu).

<sup>1</sup> These authors have contributed equally to this work.

<https://doi.org/10.1016/j.ynstr.2024.100632>

Received 19 January 2024; Received in revised form 8 March 2024; Accepted 26 March 2024

2352-2895/© 2024 The Authors. Published by Elsevier Inc. This is an open access article under the CC BY-NC-ND license (<http://creativecommons.org/licenses/by-nc-nd/4.0/>).

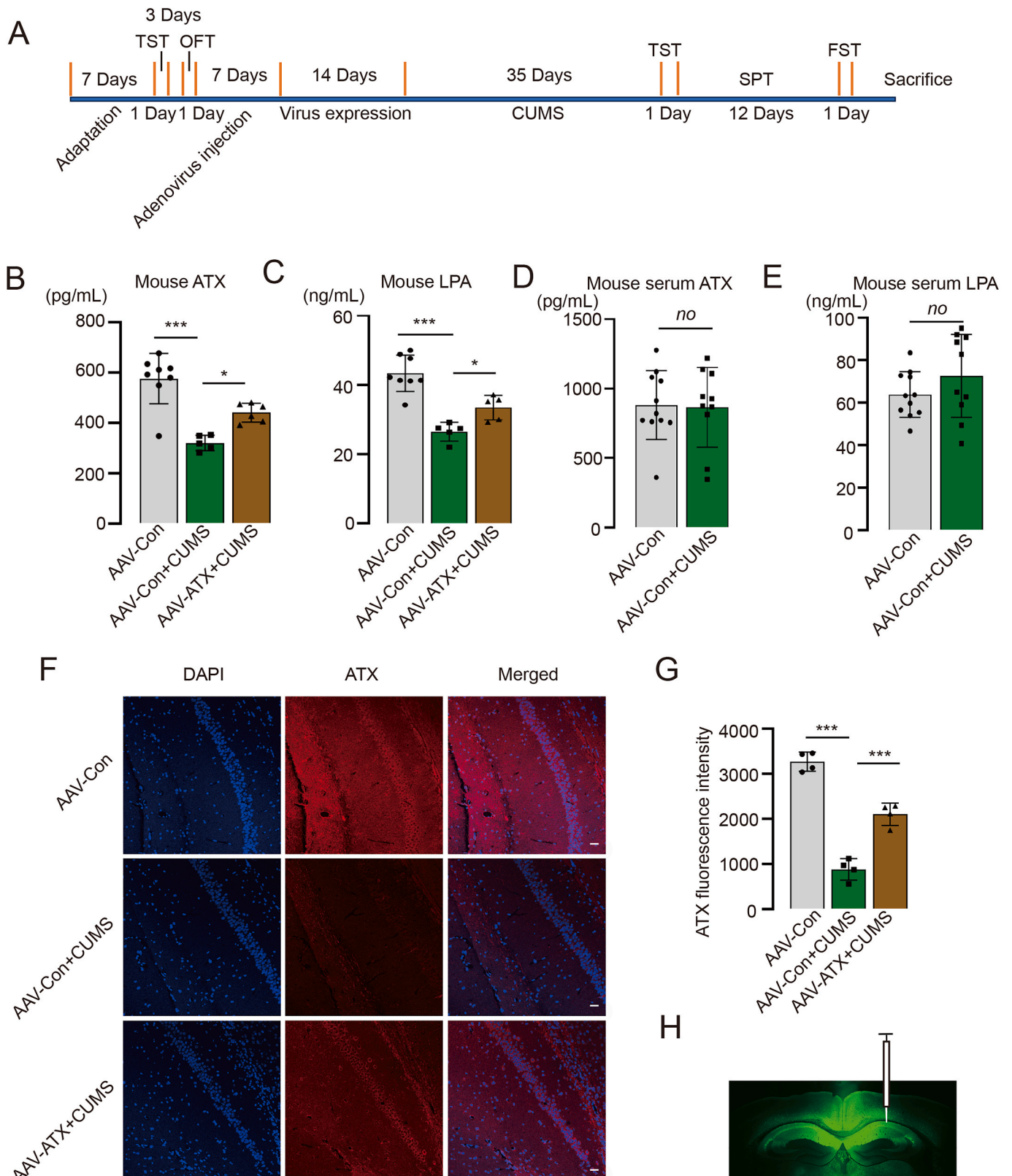
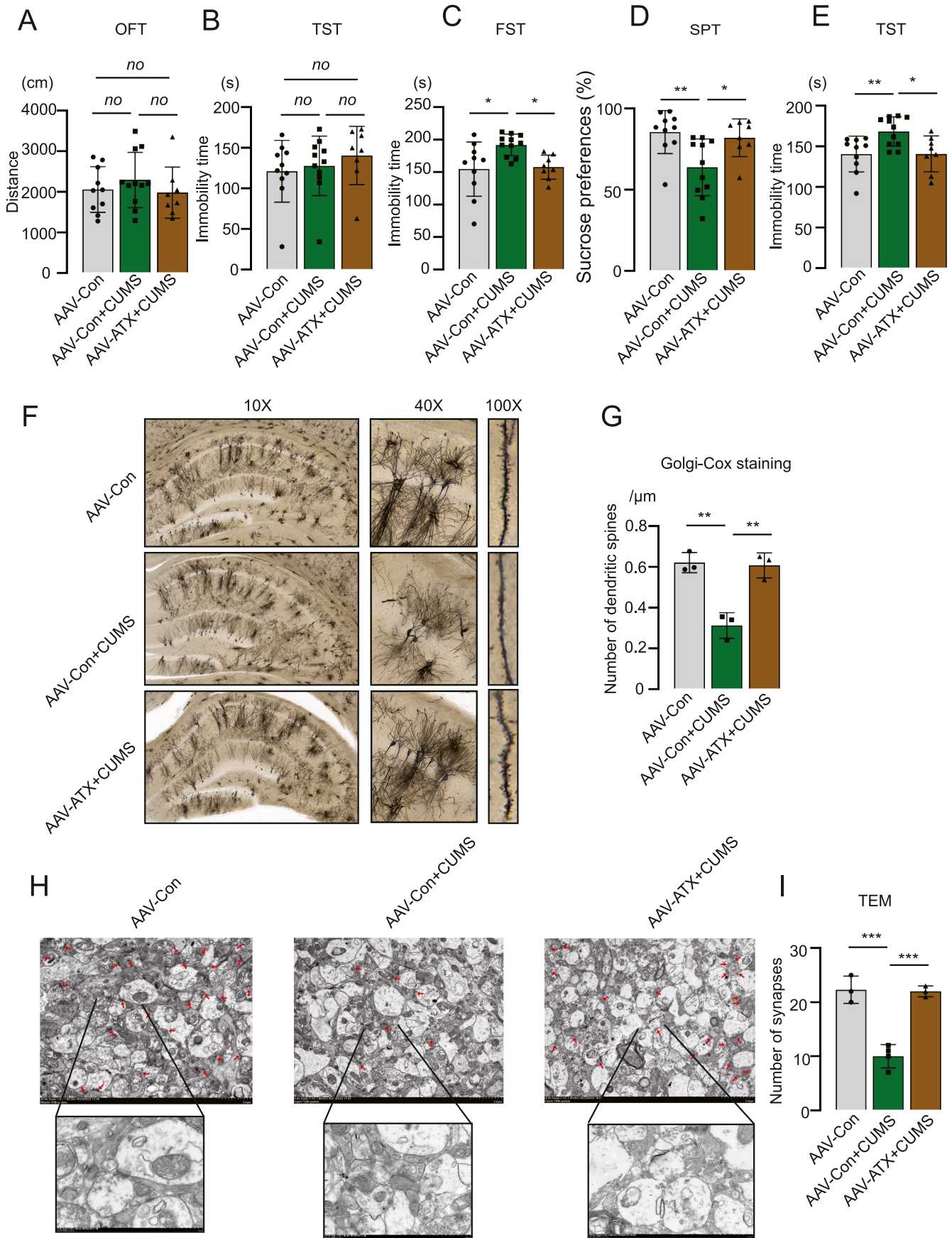


**Fig. 1.** ATX Supplementation Reverses CUMS-Induced Hippocampal ATX and LPA Reduction. The timeline illustrates the temporal nodes for virus injection and modeling procedures (A). ELISA was used to measure ATX (Kruskal-Wallis test,  $n = 5-8$ ,  $p = 0.0003$ ) and LPA (One Way ANOVA,  $n = 5-8$ ,  $F_{2,15} = 25.32$ ,  $p < 0.0001$ ) levels in the hippocampal lysates of mice from the control group, CUMS group, and CUMS plus AAV-ATX group (B–C). The ELISA results for ATX and LPA in the serum of mice from the AAV-Con group and the AAV-Con plus CUMS group are as follows (D–Two tailed  $t$ -test  $n = 10-11$   $p = 0.8988$ , E– Two tailed  $t$ -test  $n = 10-11$   $p = 0.2140$ ). Immunofluorescence analysis was conducted to assess ATX expression in the hippocampal region of mice in the control group, CUMS group, and CUMS plus AAV-ATX group (F–G, One Way ANOVA,  $n = 4$ ,  $F_{2,9} = 105.1$ ,  $p < 0.0001$ ). Scale bar: 20  $\mu\text{m}$ . The figure illustrates the site of adenovirus injection (H).



(caption on next page)

**Fig. 2.** Increasing ATX alleviates depression-like behavior and synaptic damage. The pre-injection and pre-modeling OFT result for each group (A, One Way ANOVA,  $n = 8-11$ ,  $F_{2,26} = 0.6562$ ,  $p = 0.5272$ ). The pre-injection and pre-modeling TST result for each group (B, One Way ANOVA,  $n = 8-11$ ,  $F_{2,26} = 0.6562$ ,  $p = 0.6296$ ). The results of the FST in the normal control group, the CUMS group, and the CUMS-supplemented AAV-ATX group of mice (C, One Way ANOVA,  $n = 8-11$ ,  $F_{2,26} = 5.512$ ,  $p = 0.0101$ ). SPT results of the normal control group, the CUMS group, and the CUMS-supplemented AAV-ATX group in mice (D, Kruskal-Wallis test,  $p = 0.0075$ ). The results of the TST in mice: a comparison between the normal control group, the CUMS group, and the CUMS group supplemented with AAV-ATX (E, One Way ANOVA,  $n = 8-11$ ,  $F_{2,26} = 6.166$ ,  $p = 0.0064$ ). Golgi staining showed dendritic spines in the hippocampus of the normal control group, the CUMS group, and the CUMS-supplemented AAV-ATX group (F-G, One Way ANOVA,  $n = 3$ ,  $F_{2,6} = 27.04$ ,  $p = 0.0010$ ). TEM of synaptic activity in the hippocampus of the normal control group, the CUMS group, and the CUMS-supplemented AAV-ATX group mice (H-I, One Way ANOVA,  $n = 3$  or  $4$ ,  $F_{2,7} = 43.40$ ,  $p = 0.0001$ ).

LPA synthesis, in individuals with MDD compared to healthy controls (Itagaki et al., 2019; Omori et al., 2021). Furthermore, findings from Itagaki et al. (2019) suggest that ATX levels in the serum of MDD patients increased following electroconvulsive therapy treatment, highlighting a crucial role for ATX, and consequently LPA, in the pathophysiological framework of depression.

LPA is omnipresent across all tissues studied to date (Plastira et al., 2020). The synthesis of LPA involves various enzymatic pathways, among which ATX emerges as a key enzyme. This secreted glycoprotein catalyzes the conversion of lysophosphatidylcholine (LPC) into LPA (Magkrioti et al., 2019). LPA acts as an intercellular communication mediator by attaching to G protein-coupled receptors (GPCRs) on the cell membrane (Sapkota et al., 2020). The most thoroughly researched LPA receptors thus far are LPA1 to LPA6 (Roza et al., 2019). Notably, the LPA1, LPA2, LPA4, and LPA6 receptors are present in the hippocampus (Suckau et al., 2019). Disruptions in LPA signaling are deeply intertwined with brain development and numerous neurological conditions, influencing aspects such as myelin sheath formation, synaptic activity, neural precursor cells, and brain immune function (Yung et al., 2015). LPA is directly involved in regulating the proliferation of adult hippocampal progenitor cells and neurogenesis, potentially through the AKT and MAPK pathways (Walker et al., 2016). ATX, a soluble enzyme found extracellularly, is significantly concentrated in the plasma and CSF of mammals (Herr et al., 2020). Similar to LPA, mutants lacking ATX exhibit underdeveloped vasculature, prominent neural tube defects, and asymmetrical cranial folds, highlighting the role of ATX in vascular and neuronal formation (Savaskan et al., 2007). There are also supporting data for the role of the ATX-LPA axis in advancing Alzheimer's disease (Herr et al., 2020). Both excessive and deficient ATX and LPA levels correlate with the emergence of related illnesses. Given the body's critical need for balance in its biochemical constituents for regular physiological operations, we hypothesize that reduced ATX and LPA levels have significant physiological and pathological consequences for patients with depression. Several pieces of research point to a strong link between LPA and synaptic plasticity (Roza et al., 2019; García-Morales et al., 2015; Robinson, 2015). The diminished concentrations of ATX and LPA in the brains of patients with depression might influence synaptic plasticity, thereby contributing to the onset of disease. However, no reports are showing the role of ATX and LPA in depression-like behaviors in rodents.

Hence, the current study aims to establish, using murine hippocampal cell lines and live mouse models, whether ATX and LPA induce depression by disrupting synaptic function. We also investigated whether supplementing ATX can improve synaptic function and depressive behaviors.

## 2. Methods

### 2.1. Cells

HT22 cells (mouse hippocampal neuronal cell line) were purchased from Procell Life Science & Technology Co., Ltd. Cells were cultured at 37 °C with 5% CO<sub>2</sub> in Dulbecco's modified Eagle's medium (DMEM, Gibco) supplemented with 10% fetal bovine serum (FBS, WISENT, Catalog# 086-150) and 1% penicillin/streptomycin (Gibco, Catalog# 15140-122). The processing of LPA (C<sub>21</sub>H<sub>41</sub>O<sub>7</sub>P, MedChemExpress, Catalog# HY-137862), the LPA receptor inhibitor ki16425

(MedChemExpress, Catalog# HY-13285), and the ERK (extracellular regulated protein kinases) inhibitor SCH772984 (MedChemExpress, Catalog# HY-50846) begins when the HT22 cell density reaches approximately 80%. The cellular experiments in this study involved treatment with LPA (at varying concentrations), Ki16425 (at 50 μM), and SCH772984 (at 10 μM).

### 2.2. Mice

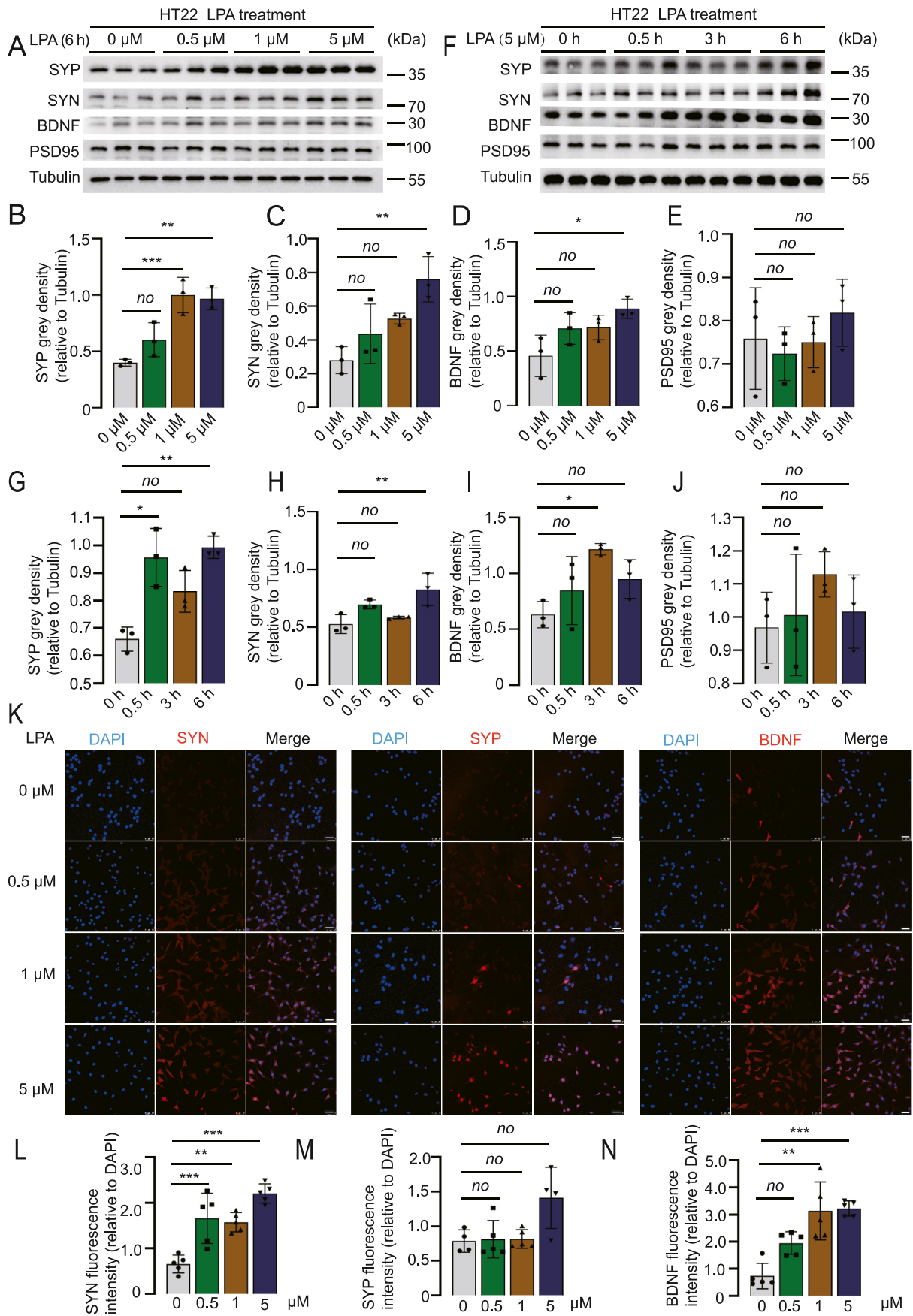
C57BL/6J (~20 g) male mice were purchased at 7 weeks of age from Hunan SJA Laboratory Animal Co., Ltd. The aforementioned mice will undergo a one-week acclimatization period in the animal facility, ensuring ample hydration and provision of sustenance with a 12 h/12 h light/dark cycle throughout. The ambient temperature was upheld within the range of 19–23 °C, while humidity levels were maintained at approximately 40–45%. The animal experiments pertinent to this study underwent ethical review and received approval from the Animal Ethics Committee. The mice were divided into three groups: 1) AAV-CON (Empty vector virus), 2) AAV-CON (Empty vector virus) plus chronic unpredictable mild stress (CUMS), and 3) ATX adeno-associated virus (AAV-ATX) plus CUMS. The procedures for handling and modeling the animals were elucidated in the subsequent sections (Fig. 1, Fig. 2, Fig. 7); However, in Figs. 5 and 6, the mice were not subjected to CUMS modeling. We have exerted maximum efforts to minimize the suffering of animals and reduce the number of animals used. Additionally, we endeavor to employ *in vivo* cell whenever feasible to conduct certain experiments. The animal study protocol was approved by the Institutional Review Board of Renmin Hospital of Wuhan University (protocol code WDRM20230603C and date of approval is June 13, 2023).

### 2.3. Chronic unpredictable mild stress (CUMS)

The procedure for CUMS was conducted following a previously described protocol (Li et al., 2021). Briefly, the mice were initially acclimated to a suitable standard laboratory housing for a week to ensure adaptation. Behavioral observations of the mice in their baseline state were conducted using open field and tail suspension experiments. The stimulation methods employed in this study are categorized into long- and short-term stimulation. The long-term stimulation-specific procedures were as follows: 24-h water deprivation period, 24-h fasting period, 24-h exposure to 45-degree tilt, 24-h empty cage condition, and 24-h exposure to specific odors. The short-term stimulation-specific procedures were as follows: tail clamping for 5 min, cool water for 5 min, oscillation for 5 min, and restraint for 6 h. Long- and short-term stimuli were selected every day for 3 consecutive days without repetition, lasting for 5 weeks.

### 2.4. Open field test (OFT)

Each mouse was placed individually in the center of a 50 × 50 × 40 cm open field chamber equipped with 16 holes in the floor. The mice were given 5 min to freely explore the open field in a quiet room after their weight was measured. The parameters evaluated included the time spent in the central and peripheral areas and the distance traveled within the central region of the chamber.



(caption on next page)

**Fig. 3.** LPA augments BDNF, SYP, and SYN expression *in vitro*. Western blot analysis showed the expression of synaptic-associated proteins (SYP, SYN, BDNF, PSD95) in HT22 cells treated with different concentrations of LPA (A, B-One Way ANOVA,  $F_{3,8} = 17.63$   $p = 0.0007$ , C-One Way ANOVA,  $F_{3,8} = 8.536$   $p = 0.0071$ , D-One Way ANOVA,  $F_{3,8} = 4.880$   $p = 0.0325$ , E-One Way ANOVA,  $F_{3,8} = 0.7075$   $p = 0.5740$ ). Western blot analysis was performed to assess the expression of synaptic-associated proteins (SYP, SYN, BDNF, PSD95) in HT22 cells treated with LPA for varying durations (F, G- Kruskal-Wallis test,  $p = 0.0044$ , H-One Way ANOVA,  $F_{3,8} = 7.556$   $p = 0.0101$ , I-One Way ANOVA,  $F_{3,8} = 5.074$   $p = 0.0295$ , J-One Way ANOVA,  $F_{3,8} = 0.9262$   $p = 0.4712$ ). Immunofluorescence display of synaptic-associated protein expression (SYN, SYP, BDNF) in HT22 cells under different concentrations of LPA (K, L-One Way ANOVA,  $F_{3,16} = 19.14$   $p < 0.0001$ , M-One Way ANOVA,  $F_{3,8} = 5.143$   $p = 0.0132$ , N-Kruskal-Wallis test,  $p = 0.0024$ ). The scale bar positioned in the lower right corner of the image corresponds to a length of 50  $\mu\text{m}$ .

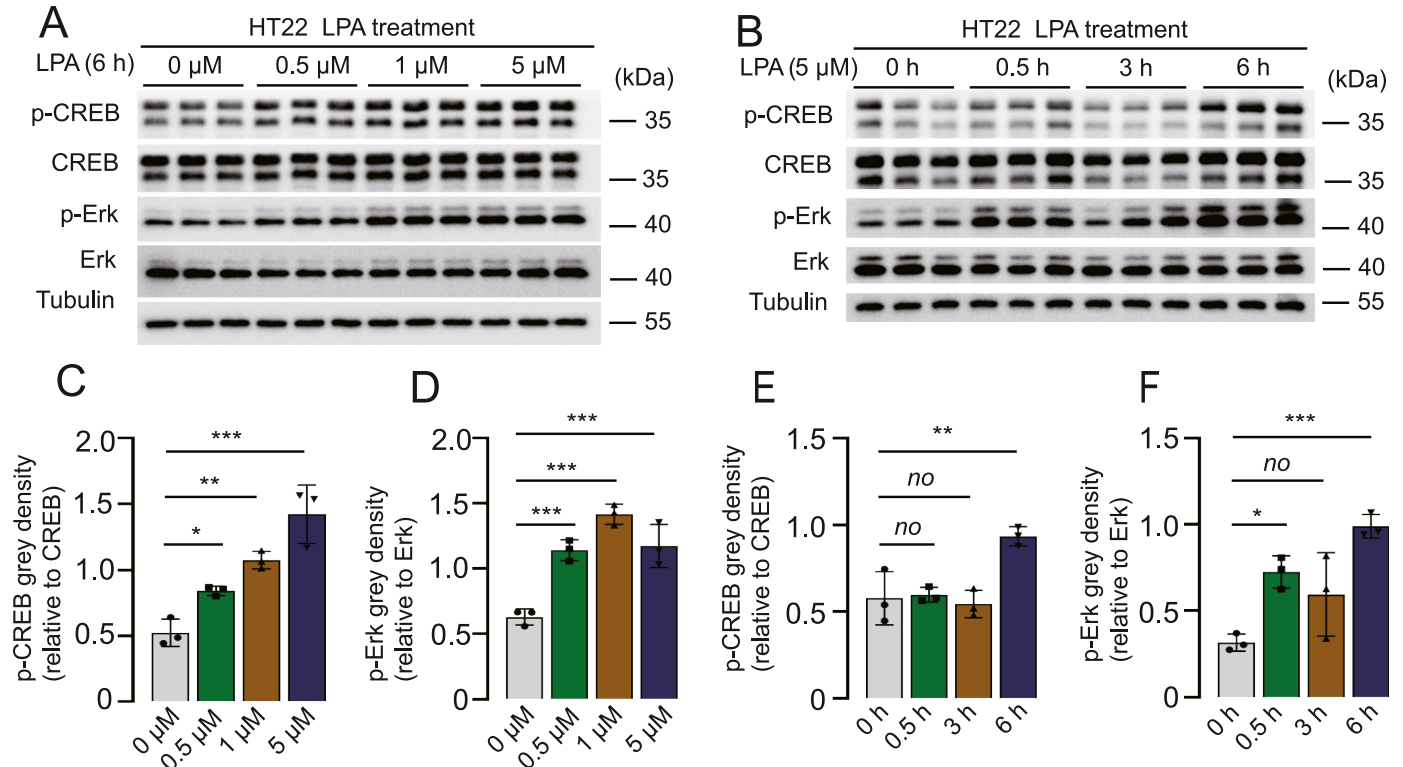


**Fig. 4.** LPA enhances BDNF/SYP/SYN expression via the ERK/CREB signaling pathway. Western blot analysis of the effects of different concentrations of LPA on the ERK/CREB signaling pathway in HT22 cells (A, C-One Way ANOVA,  $F_{3,8} = 26.30$   $p = 0.0002$ , D-One Way ANOVA,  $F_{3,8} = 30.21$   $p = 0.0001$ ). Western blot analysis of the effects of LPA treatment with varying durations on the ERK/CREB signaling pathway in HT22 cells (B, E-One Way ANOVA,  $F_{3,8} = 11.51$   $p = 0.0028$ , F-One Way ANOVA,  $F_{3,8} = 12.77$   $p = 0.0020$ ).

## 2.5. Forced swim test (FST)

Following a previously published protocol, swimming sessions were performed using cylindrical containers (30 cm height  $\times$  10 cm diameter) filled with 25  $^{\circ}\text{C}$  water to a depth of 20 cm, preventing the mice from touching the bottom with their feet. The FST lasted for 6 min, during which the immobility time was measured and recorded in the last 4 min.

## 2.6. Tail suspension test (TST)

Mice were suspended individually by their tails to a vertical bar located at the top of a box measuring 30  $\times$  30  $\times$  30 cm. To ensure stability, adhesive medical tape was attached 2 cm away from the tail tip. The duration of immobility time was measured during a 6-min testing session in the last 4 min. Immobility in the TST was defined as the absence of any limb or body movements, except those resulting from respiration.

## 2.7. Sucrose preference test (SPT)

For the SPT, the mice underwent a 96-h training period before the test to become accustomed to a 1% sucrose solution (w/v). Initially, two water bottles were provided in each cage for 24 h, followed by the introduction of two bottles of 1% sucrose solution in each cage. After an

additional 24 h, one bottle with 1% sucrose was replaced with tap water for 12 h, and then the positions of the bottles were switched. Following the adaptation period, mice were deprived of water for 24 h. Subsequently, the sucrose preference test was conducted, where mice were individually housed and offered two bottles: one containing 200 ml of 1% sucrose solution (w/v) and the other containing 200 ml of water. After 24 h, the sucrose preference was calculated as the percentage of consumed 1% sucrose solution relative to the total liquid intake.

## 2.8. Lateral ventricle injection and hippocampus injection

Following isoflurane anesthesia, the mice had their head hair shaved and securely positioned on a stereotaxic injection device. The skin was incised to separate the subcutaneous tissue and expose the anterior fontanelle, which served as the origin for the coordinates. The lateral ventricle site (X:  $\pm 1.0$  mm, Y:  $-0.3$  mm, Z:  $-2.3$  mm) and the hippocampus site (X:  $\pm 1.5$  mm, Y:  $-2.06$  mm, Z:  $-1.85$  mm) were identified. After intraperitoneal injection of the LPA receptor inhibitor Ki16425 (Sánchez-Marín et al., 2018) (30 mg/kg) for 30 min, the needle was inserted slowly, and 300  $\mu\text{M}/5 \mu\text{l}$  solution of LPA (C21H41O7P) dissolved in anhydrous ethanol was injected bilaterally into the lateral ventricles. The control group received an equimolar injection of anhydrous ethanol. The aforementioned treated mice did not undergo CUMS modeling (Figs. 5–6). CMV-betaGlobin-MCS-3Flag-autotaxin ( $1.4 \times 10^{12}$

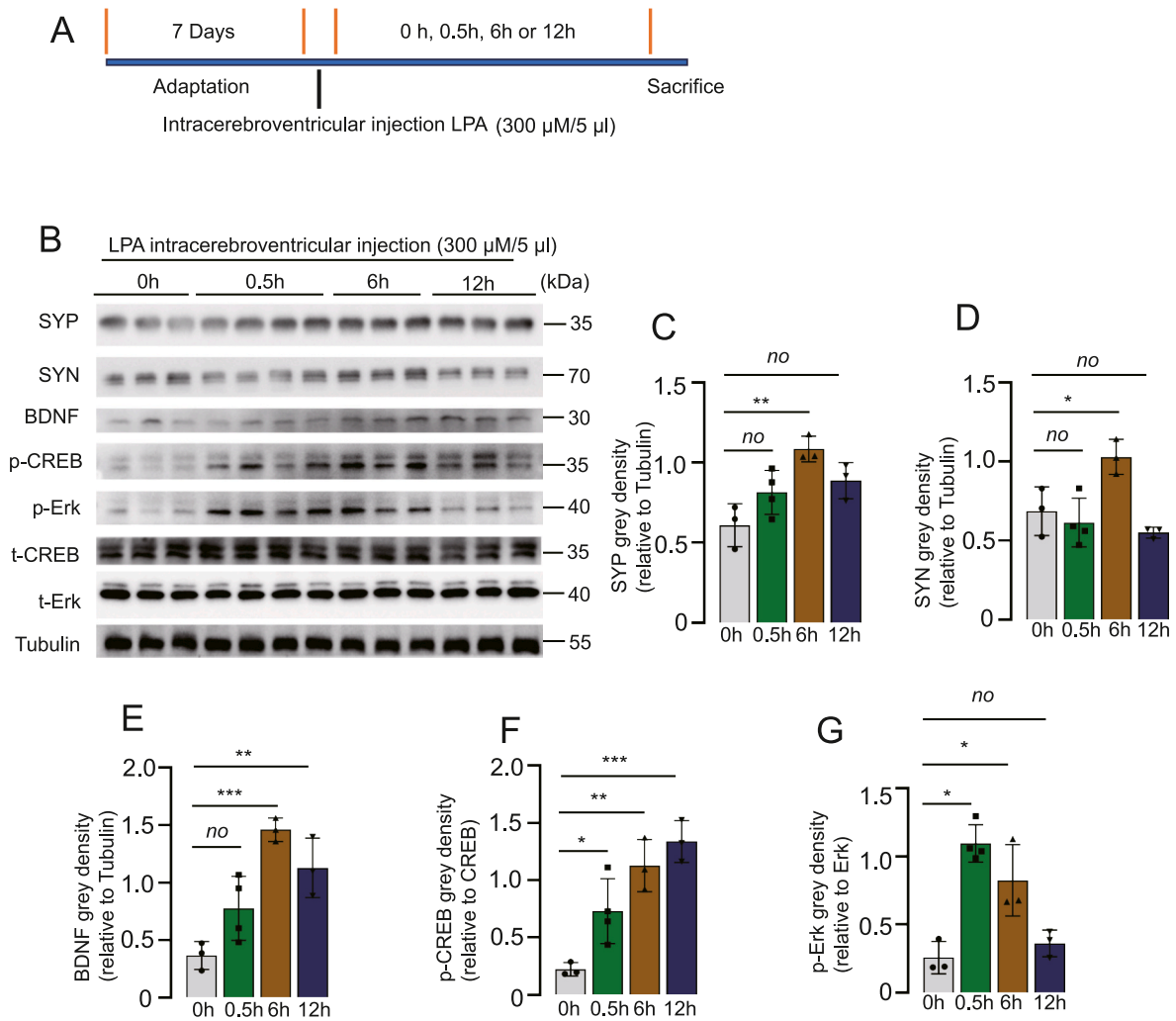


**Fig. 5.** LPA increases BDNF/SYP/SYN expression *in vivo* through the ERK/CREB pathway. Illustration of the temporal nodes for LPA injection (A). Western blot analysis showed that in the brains of mice, LPA injection into the lateral ventricles affected the expression of synaptic-related proteins in the hippocampus (B–E) (C-Kruskal-Wallis test,  $p = 0.0071$ , D-One Way ANOVA,  $F_{3,9} = 8.741$   $p = 0.0050$ , E-One Way ANOVA,  $F_{3,9} = 14.52$   $p = 0.0009$ ). Western blot showing the effect of LPA injected into lateral ventricles on the ERK/CREB signaling pathway in the hippocampus in mice (B, F–G) (F-One Way ANOVA,  $F_{3,9} = 15.76$   $p = 0.0006$ , G-Kruskal-Wallis test,  $p = 0.0023$ ).

v.g/ml) (AAV-ATX) was injected into the hippocampus, with a volume of 500 nl administered on each side. It is important to emphasize that the injection should be performed at a slow rate. The mice underwent CUMS modeling after adenovirus injection (Figs. 1, Fig. 2, Fig. 7).

## 2.9. Paraffin sections

After anesthetization, the mice were euthanized, and 0.9% physiological saline and 4% paraformaldehyde were utilized for cardiac perfusion. Fresh tissue was collected and promptly placed in tissue fixative for a minimum of 24 h. Subsequently, the tissues were dehydrated using a dehydration machine and an alcohol gradient. For paraffin embedding and sectioning, the wax-soaked tissue was placed in the embedding machine before transferring the trimmed wax block to the paraffin sectioning machine for sectioning at a thickness of 4 μm.

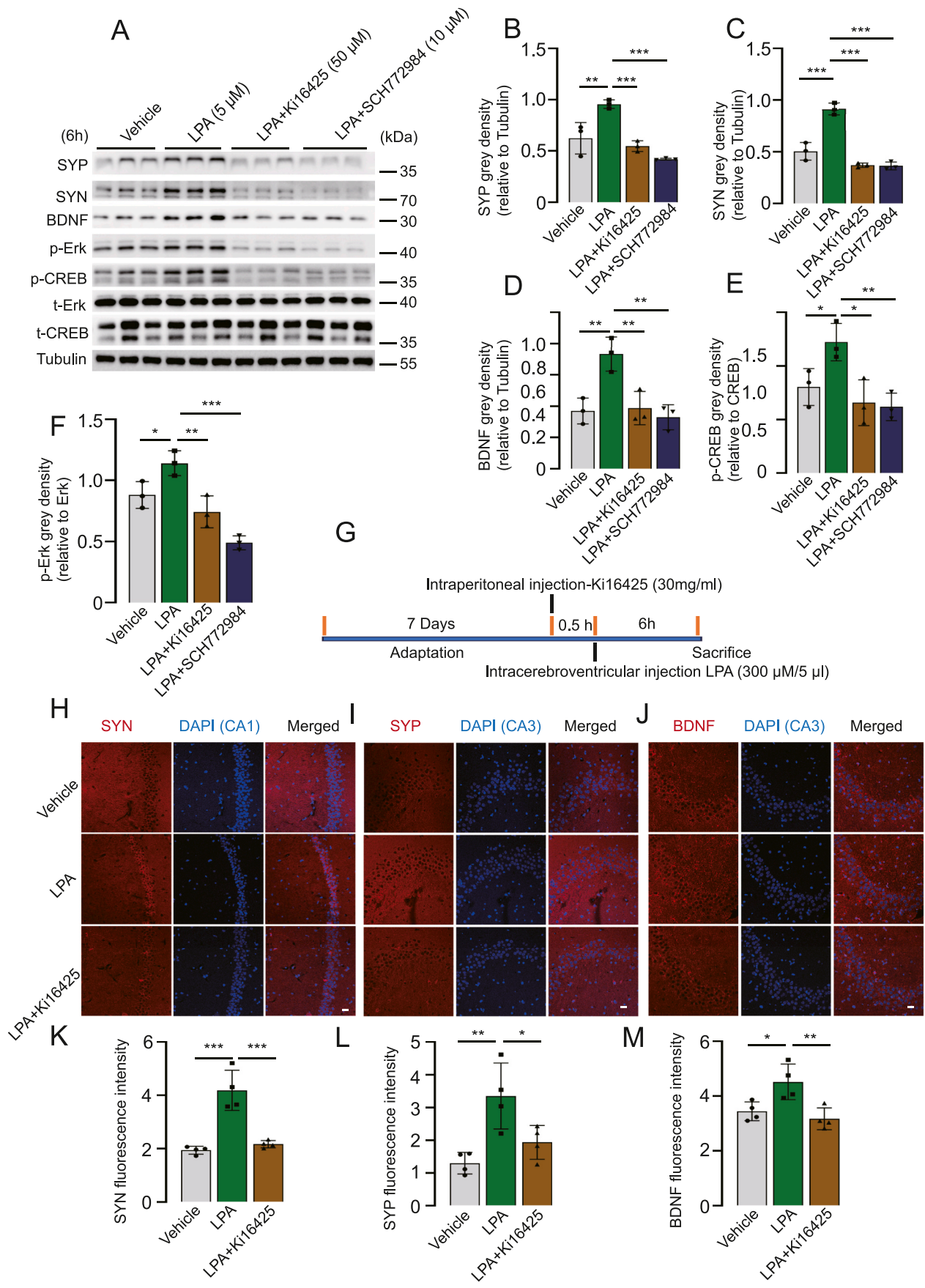
## 2.10. Immunofluorescence

The paraffin sections were dewaxed by immersing them in xylene solution three times, with each immersion lasting 25 min. Subsequently, the sections were immersed in the following sequence: absolute ethanol, 95% ethanol, 85% ethanol, 75% ethanol, and ultrapure water, with each

immersion lasting 5 min. The brain slice was then submerged in Trisodium citrate solution at 94 °C for 20 min to facilitate antigen retrieval before allowing the slice to naturally cool to room temperature. The processed brain slices or cell slides fixed with 4% PFA were washed three times with phosphate buffered saline (PBS) and sealed at room temperature for 1 h with 3% BSA containing 3 Triton-X 100. A circle was drawn around the brain slice using a hydrophobic pen before incubation with antibodies (Synapsin-I 1:200, Abclone; Synaptophysin 1:200, Proteintech; BDNF 1:200, Abcam; LPA 1:200, Echelon; ATX 1:200, Abclone) at 4 °C for a minimum of 24 h. After incubation, the slides were washed five times with PBS and incubated with the fluorescent secondary antibody (1:500, Proteintech) at room temperature for 2 h. Following another five washes with PBS, sealing agent was added dropwise (Abcam 104139) to the glass slide for sealing. Finally, images of the brain slices were captured using a fluorescence microscope (Leica-DMi8).

## 2.11. Enzyme-linked immunosorbent assay (ELISA)

The levels of LPA and ATX were measured using ELISA kits (Bio-swamp, Catalog# LPA- MU30816 and ATX- MU30993) following the manufacturer's instructions. Initially, the tissue samples were washed



(caption on next page)

**Fig. 6.** Reduction of BDNF/SYP/SYN expression by inhibiting the LPAR/ERK/CREB signaling pathway. Western blot analysis showed the expression of synaptic-related proteins (SYP, SYN, BDNF) in HT22 cells treated with different groups (Vehicle, LPA, Ki16425, SCH72984) (A, B-One Way ANOVA,  $F_{3,8} = 22.27$   $p = 0.0003$ , C-One Way ANOVA,  $F_{3,8} = 64.40$   $p < 0.0001$ , D-One Way ANOVA,  $F_{3,8} = 126$   $p < 0.0001$ ). Western blot showing the effects of different treatment groups (Vehicle, LPA, Ki16425, SCH72984) on ERK/CREB in HT22 cells (A, E-One Way ANOVA,  $F_{3,8} = 7.482$   $p = 0.0104$ , F-One Way ANOVA,  $F_{3,8} = 20.70$   $p = 0.0004$ ). The timeline depicts the temporal nodes for LPA intracerebroventricular injection and Ki16425 administration (G). Immunofluorescence showed the effect of different treatment groups (Vehicle, LPA Lateral ventricles injection, LPA Lateral ventricles injection plus Ki16425 intraperitoneal injection) on the expression of synaptic-related proteins in the hippocampus of mice (H–J). Immunofluorescence analysis was conducted to assess SYN, SYP, BDNF expression in the hippocampal region of mice in the Vehicle group, LPA group, and LPA plus Ki16425 group (K-One Way ANOVA,  $n = 4$ ,  $F_{2,9} = 30.10$ ,  $p = 0.0001$ , L-One Way ANOVA,  $n = 4$ ,  $F_{2,9} = 9.491$ ,  $p = 0.0061$ , M-One Way ANOVA,  $n = 4$ ,  $F_{2,9} = 9.584$ ,  $p = 0.0059$ ). Scale bar: 20  $\mu\text{m}$ .

with PBS (0.01 M, pH 7.4) to remove surface impurities before weighing and finely mincing them for efficient homogenization. The tissue was combined with prechilled PBS (with added protease inhibitor), maintaining a 1:9 tissue weight to PBS volume ratio (e.g., 1 g of tissue sample corresponds to 9 ml of PBS). The mixture was then homogenized on ice or in a cold bath, followed by centrifugation at 4 °C for 5–10 min at 5000 $\times$ g to collect the supernatant. Protein content was determined using the BCA method and adjusted to a uniform total protein concentration. Next, diluted standards were prepared at concentrations of 640, 320, 160, 80, 40, and 0 pg/ml. Subsequently, 50  $\mu\text{l}$  of each standard was added sequentially before carefully adding the sample to the bottom of each well in the enzyme-labeled plate, taking care to avoid touching the well walls. The plate was shaken gently to ensure thorough mixing of the sample before proceeding with the sequential steps of enzyme addition, incubation, solution preparation, washing, color development, termination, and determination.

## 2.12. Golgi-cox staining

The mice were euthanized, and the samples were collected and fixed. The brain tissue was harvested and immersed in a fixation solution for at least 48 h. Mouse brain tissue was sliced into 2–3-mm blocks and rinsed with physiological saline. The tissue blocks were transferred to a round-bottomed EP tube and submerged in Golgi staining solution for 14 days. Distilled water was used to perform three rinses before overnight immersion in 80% glacial acetic acid to soften the tissue. After rinsing with distilled water, the tissue was placed in a 30% sucrose solution. Using an oscillating slicer, the tissue was cut into 100- $\mu\text{m}$  sections and affixed to gelatin-coated slides. The sections were left to air dry in the dark overnight. Subsequently, the dried tissue slides were treated for 15 min with concentrated ammonia water, followed by a 1-min rinse with distilled water. An acidic hardening fixing solution was applied for 15 min, followed by a 3-min distilled water wash. Finally, the slides were dried and sealed with glycerol gelatin. Power on the histological slide scanner and launch the Panoramic Scanner software. Utilize automatic or manual methods to identify the scanning area. Opt for the depth-of-field expansion scanning mode. The scanner will autonomously focus and capture composite images. Select intact secondary branches with clearly visible dendritic spines at the apex of the CA1 region in the hippocampal tissue. Analyze five neurons per hippocampal tissue slice.

## 2.13. Transmission electron microscopy (TEM) staining

First, we selected an appropriate sampling site for fresh tissue to minimize mechanical damage, such as traction, contusion, and compression. The tissue samples were collected within a time frame of 1–3 min, ensuring a sample size of 1  $\text{mm}^3$ . Then, 1% osmic acid prepared with 0.1 Phosphate buffer PB (pH 7.4) was added to fix the tissue in the dark at room temperature for 2 h. Thereafter, room temperature dehydration, osmotic embedding, polymerization, ultrathin sectioning, staining, and finally observation under TEM (Hitachi- HT7800/HT7700) were performed to collect images for analysis.

## 2.14. Western blot

Cells or mouse hippocampal tissues were lysed using RIPA buffer

(Servicebio) supplemented with protease and phosphatase inhibitors (MedChemExpress). Subsequently, the tissue lysate was transferred into an ultrasonic cell pulverizer and centrifuged at 13,200 rpm for 25 min at 4 °C. After centrifugation, the supernatant was collected, and the protein concentration was measured using the BCA method to determine the appropriate amount of protein sample to be used. The recommended protein loading volume is within the range of 5–20  $\mu\text{g}$ . The protein samples were then transferred onto a PVDF membrane (Millipore). We then performed the sealing step using a 5% BSA solution before immersing the membrane in the primary antibody solution at 4 °C overnight. The following antibodies were used: Synapsin-I (SYN, 1:4000, Abclone), Synaptophysin (SYP, 1:4000, Proteintech), Brain-derived neurotrophic factor (BDNF, 1:2000, Abcam), Postsynaptic density protein 95 (PSD95, 1:4000, Proteintech),  $\beta$ -Tubulin (1:10000, HUABIO), p-ERK (1:1000, Cell Signaling Technology), ERK (1:2000, Cell Signaling Technology), p-CREB (1:1000, Cell Signaling Technology), and CREB (1:2000, Cell Signaling Technology). The next day, the membrane was rinsed with TBST 4 times, with each rinse lasting 5 min. Subsequently, the membrane was incubated with the secondary antibody (mouse or rabbit antibody, 1:8000, SAB) at room temperature for 1 h. Finally, the membrane was washed six times with TBST and developed using a chemiluminescence instrument.

## 2.15. Statistical analysis

All quantitative data are presented as the mean  $\pm$  standard error of the mean (s.e.m.). When the data adheres to normality distribution and homogeneity of variance, statistical analysis was conducted using Two-tailed *t*-test or one-way analysis of variance (ANOVA) by the LSD test for post hoc comparisons. Conversely, when such assumptions are not satisfied, non-parametric tests (Kruskal-Wallis test) are employed. Differences with *P* values  $< 0.05$  were considered to be statistically significant (\**P*  $< 0.05$ , \*\**P*  $< 0.01$ , \*\*\**P*  $< 0.001$ ).

## 3. Results

### 3.1. ATX supplementation reverses CUMS-induced hippocampal ATX and LPA reduction

The illustration depicts the temporal nodes of adenovirus injection and chronic unpredictable mild stress (CUMS) modeling in this study (Fig. 1A). Given the findings of previous studies indicating a reduction in ATX and LPA levels in the serum and CSF of individuals with depression (Omori et al., 2021), we investigated alterations in ATX and LPA levels within the hippocampus of mice with or without CUMS. The ELISA findings indicated lower ATX and LPA levels in the hippocampus of mice in the CUMS group compared to those in the control group, while the AAV-ATX injection group exhibited elevated levels of ATX and LPA compared to those in the CUMS group (Fig. 1B–C). We also assessed the levels of ATX and LPA in the serum of mice from the AAV-Con group and the AAV-Con plus CUMS group (Fig. 1D–E). Simultaneously, our immunofluorescence results indicated that the CUMS group had lower ATX levels than the control group, whereas the CUMS plus AAV-ATX injection group had higher ATX levels (Fig. 1F–G). The following figure illustrates the site of adenovirus injection (Fig. 1H).

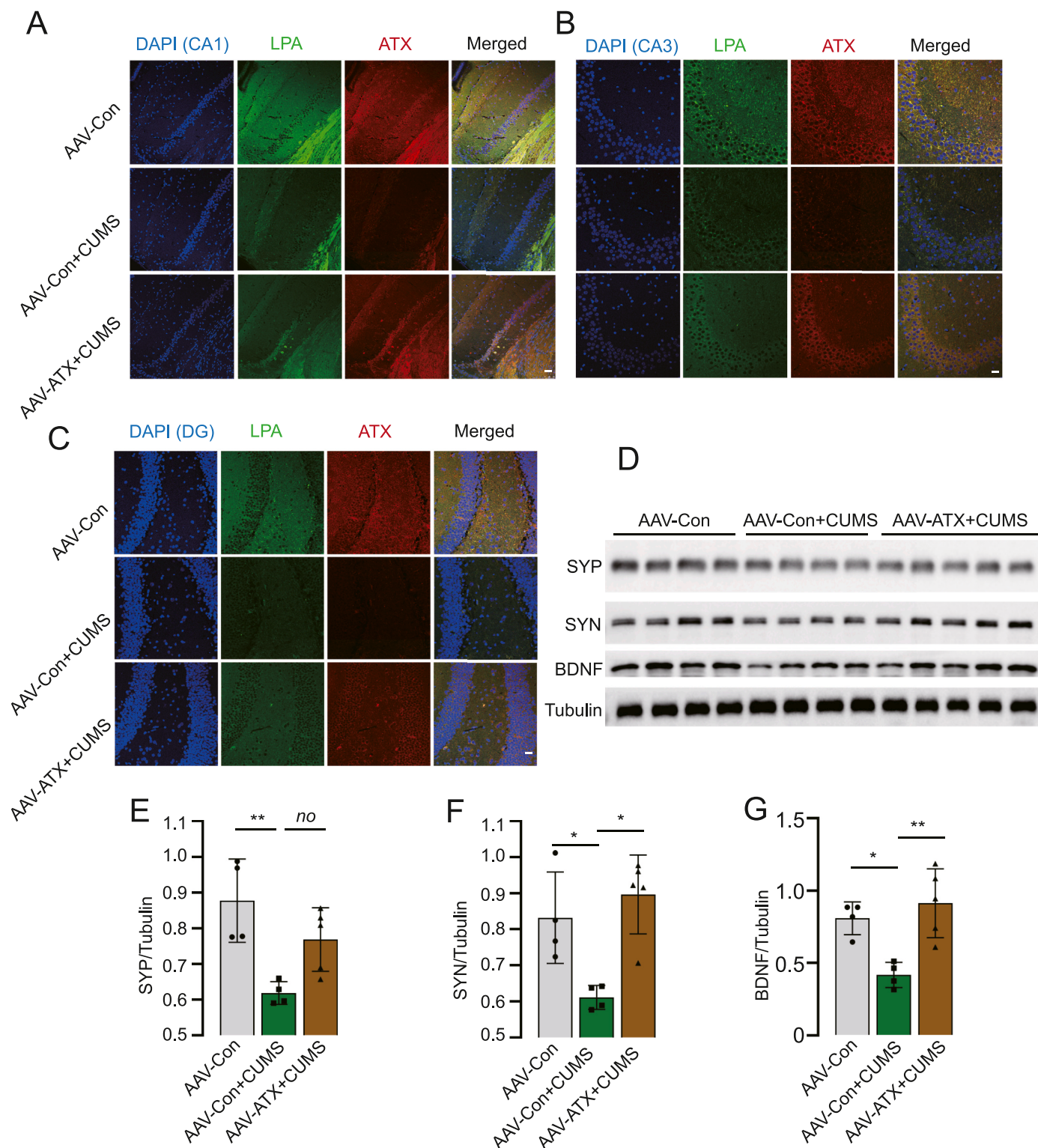


**Fig. 7.** Elevating ATX expression in the hippocampus boosts synaptic-related protein expression. Immunofluorescence display of LPA and ATX expression in the hippocampus of different groups of mice (Control group, CUMS group, CUMS plus AAV-ATX group) (A–C). Western blot showing the expression of synaptic-related proteins in the hippocampus of different groups of mice (control group, CUMS group, CUMS plus AAV-ATX group) (D, E–One Way ANOVA,  $F_{2,10} = 8.917$   $p = 0.0060$ , F-Kruskal-Wallis test,  $p = 0.0083$ , G–One Way ANOVA,  $F_{2,10} = 10.16$   $p = 0.0039$ ). Scale bar: 20  $\mu$ m.

### 3.2. Increasing ATX alleviates depression-like behavior and synaptic damage

We observed that the administration of ATX in the hippocampal region of mice effectively improved depression-like behavior. Before

virus injection and modeling, there were no significant differences in the total distance traveled by mice in the OFT among the various groups, indicating no discernible disparities in locomotor abilities among the groups of mice (Fig. 2A). There were also no significant differences observed in the immobility time during the tail suspension test among

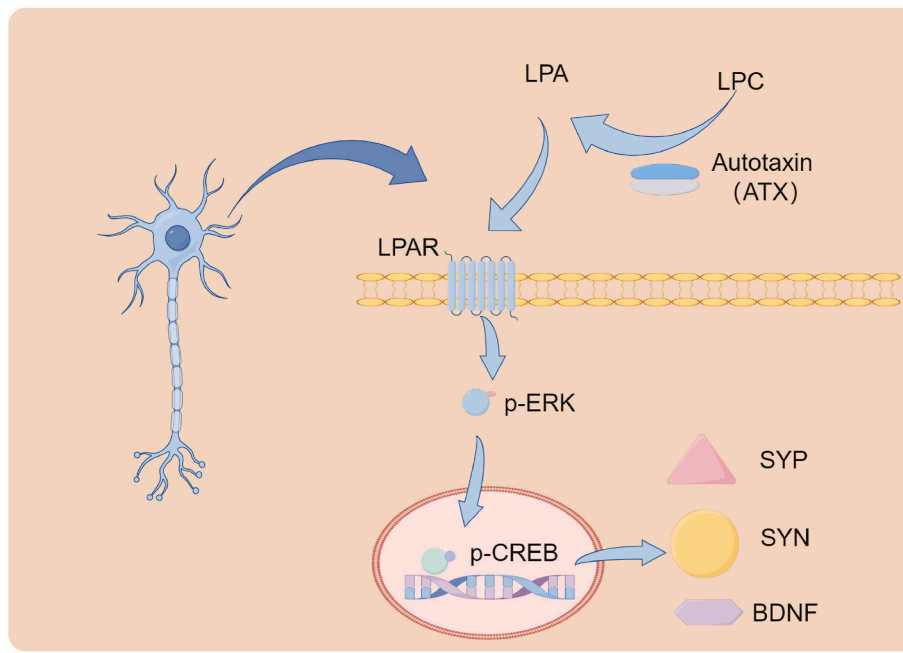


**Fig. 8.** Illustration of the ATX-LPA signaling pathway in depression (by Figdraw). LPC (lysophosphatidylcholine), LPA (lysophosphatidic acid), LPAR (lysophosphatidic acid receptor), SYP (synaptophysin), SYN (synapsin-I), BDNF (brain-derived neurotrophic factor).

the various groups of mice before virus injection (Fig. 2B). During the forced swimming experiment after CUMS, we noted a significant decrease in the duration of immobility behavior in the CUMS group supplemented with ATX compared to the CUMS group alone (Fig. 2C). Similarly, in both the sugar preference and tail suspension tests, we observed a consistent pattern in that the CUMS group supplemented with ATX exhibited a higher preference for sugar water intake (Fig. 2D) and an decreased duration of immobility compared to the CUMS group (Fig. 2E). Regarding synapses, our observations from Golgi staining revealed a significant increase in the ratio of dendritic spines to dendritic length in the CUMS group supplemented with ATX compared to the CUMS group (Fig. 2F–G). The results obtained by TEM indicated a significant reduction in the number of synapses within the CUMS group compared to the control group. Conversely, the CUMS plus AAV-ATX group exhibited a considerable increase in the number of synapses compared to the CUMS group (Fig. 2H and I).

### 3.3. LPA augments BDNF, SYP, and SYN expression in vitro

Considering the impact of the ATX–LPA axis on synapses, we conducted further research to investigate whether LPA enhances the expression of proteins associated with synapses. As depicted in Fig. 3A, the expression of SYN, SYP, and BDNF in HT22 cells increased upon diverse concentrations LPA treatment. However, LPA did not elicit any notable effect on the expression of PSD95. The statistical diagram illustrating the relevant changes is shown in Fig. 3B–E. Similarly, through western blotting, we observed that LPA with varying durations also increased the expression of BDNF, SYP, and SYN in HT22 cells (Fig. 3F). The corresponding statistical diagram is shown in Fig. 3G–J. Moreover, using immunofluorescence, we detected consistent changes where LPA augmented the expression of BDNF, SYP, and SYN in HT22 cells (Fig. 3K). The statistical diagram is shown in Fig. 3L–N.

### 3.4. LPA enhances BDNF/SYP/SYN expression via the ERK/CREB signaling pathway in vitro and in vivo

To delve deeper into the specific mechanism underlying the promotion of synaptic-associated protein expression by LPA, we

investigated potential changes in signaling pathways associated with protein production. Western blotting demonstrated that LPA can activate the ERK/CREB signaling pathway in HT22 cells (Fig. 4A–B). The correlation statistics depicting the dose-dependent relationship between p-CREB and p-ERK with LPA are shown in Fig. 4C and D, and the correlation statistics illustrating the time-dependent relationship between p-CREB and p-ERK with LPA are shown in Fig. 4E and F. Previous research has suggested that the production of BDNF, SYP, and SYN is associated with the activation of the ERK/CREB signaling pathway (Yao et al., 2022; Xue et al., 2009; Guo et al., 2020). Therefore, we speculate that LPA enhances the expression of synaptic-related proteins by activating the ERK/CREB signaling pathway. The aforementioned research primarily focused on the cellular level. Subsequently, we conducted further investigations to examine the impact of LPA on synaptic-related proteins and associated signaling pathways in the mouse hippocampus, to determine whether the results were similar to those observed in isolated somatic cells. The concluding timeline presents the temporal nodes for LPA injection in the context of these results (Fig. 5A). Following the administration of LPA into the lateral ventricles, western blot analysis revealed a notable increase in synapse-related proteins in the mouse hippocampus (Fig. 5B–E), together with activation of the ERK/CREB pathway (Fig. 5B, F–G).

### 3.5. Reduction in BDNF/SYP/SYN expression by inhibiting the LPAR/ERK/CREB signaling pathway

The abovementioned research suggests that LPA enhances the expression of synaptic-related proteins through the activation of the ERK/CREB signaling pathway. To investigate further, we explored whether the effects of LPA could be hindered by inhibiting the activation of ERK/CREB. In HT22 cells, western blot analysis demonstrated a noteworthy reduction in synaptic-associated proteins in both the LPA plus LPA receptor 1/3 inhibitor (Ki16425) group and the ERK inhibitor (SCH772984) group compared to the LPA group (Fig. 6A–D). Moreover, the ERK/CREB signaling pathway exhibited significant inhibition in these groups (Fig. 6A–E, F). We also conducted a verification experiment on animals. The concluding timeline illustrates the temporal nodes for LPA intracerebroventricular injection and Ki16425 intraperitoneal

injection in this study (Fig. 6G). The immunofluorescence results indicated a significant increase in the expression of SYN in the CA1 region, SYP in the CA3 region, and BDNF in the CA3 region of the mouse hippocampus following LPA injection into the lateral ventricles. In contrast, the expression of SYN, SYP, and BDNF in the LPA plus Ki16425 intraperitoneal injection group exhibited a notable decrease compared to that in the LPA injection group (Fig. 6H–J). The fluorescence statistics are illustrated in the accompanying figure (Fig. 6K–M).

### 3.6. Increased ATX expression in the hippocampus boosts synaptic-related protein expression

Subsequently, we investigated whether supplementation of ATX in the hippocampus of mice could ameliorate depressive-like behavior by enhancing the expression of synaptic-related proteins. Using immunofluorescence, we observed a substantial elevation of LPA and ATX in the CA1, CA3, and DG regions of the hippocampus in the CUMS plus AAV-ATX group, in contrast to the CUMS group (Fig. 7A–C). The western blot results revealed a significant decrease in SYP, SYN and BDNF levels in the hippocampus of the CUMS group compared to the control group (Fig. 7D–G). Conversely, the hippocampus of the CUMS plus AAV-ATX injection group exhibited a remarkable increase in SYN and BDNF expression compared to the CUMS group (Fig. 7D, F, G). Regrettably, we observed an increase in SYP levels in the CUMS plus ATX injection group compared to the CUMS group, albeit with no significant differences (Fig. 7E).

## 4. Discussion

Our findings indicate that the reduction in ATX and LPA levels induces changes in the expression of proteins linked to synaptic plasticity both *in vitro* and *in vivo*, including SYN, SYP, and BDNF. Furthermore, we identified the involvement of the ERK/CREB signaling pathway in mediating the effects of ATX and LPA. Notably, targeted supplementation of ATX significantly alleviated depression-like behaviors. This study suggests that the ATX-LPA pathway could impact depression-like behaviors by regulating synaptic plasticity in the brains of mice exposed to CUMS.

The observation of reduced ATX and LPA levels in mouse hippocampal lysates (Fig. 1B–C) prompted us to investigate the potential advantages of ATX supplementation. Interestingly, no changes in ATX and LPA were observed in the murine serum, which could potentially be attributed to the presence of the blood-brain barrier (Fig. 1D–E). Previous research has shown that ATX inhibitors can decrease spontaneous postsynaptic currents, thereby influencing synaptic function (Vogt et al., 2016). Simultaneously, the LPA/LPAR (LPA receptor) signaling pathway has been reported to be associated with alterations in glutamate transmission and synaptic plasticity (Roza et al., 2019; Peñalver et al., 2017). Given prior research on the relationship between ATX-LPA and synaptic plasticity, we further explored the potential impact of ATX-LPA on synaptic plasticity in depression. Our results showed that ATX supplementation effectively mitigated depressive-like behavior and synaptic impairment (Fig. 2). In terms of the specific mechanisms through which LPA impacts neural cells, we found that LPA significantly boosts the synthesis of various synaptic-related proteins (SYP, SYN, BDNF) *in vitro* and *in vivo*. Evidence from two perspectives confirmed that LPA can enhance the expression of synaptic-related proteins. While existing research confirms LPA's ability to promote BDNF expression (Fujita et al., 2008), there has been sparse investigation into LPA's effects on synaptic plasticity beyond its known influences on BDNF expression. Our study further illuminates LPA's role in synaptic plasticity. Considering the unique properties of SYP (Thiel and Synapsin, 1993) and SYN (Shupliakov et al., 2011), LPA may notably affect synaptic vesicle operations. Following the validation of the abovementioned research findings, we did not confine ourselves solely to studying the relationship between LPA and synaptic-related proteins. Instead, we further explored

the molecular mechanisms by which LPA enhances the expression of synaptic-related proteins.

In light of the phenomena previously discussed, we delved into the potential mechanisms by which LPA might stimulate the production of synaptic-related proteins. Our *in vivo* and *in vitro* experiments confirmed that ATX and LPA could promote the formation of these proteins through the ERK/CREB signaling pathway. Various studies have documented that activating the ERK/CREB signaling pathway can alleviate neuroinflammation and nerve damage, resulting in antidepressant-like effects (Yan et al., 2020; Zhang et al., 2020; Jiang et al., 2021; Li et al., 2019), providing additional validation for our conclusions. We extended our research to examine the potential impact of ATX supplementation on depression-like behaviors *in vivo*. The findings revealed that ATX supplementation significantly increased the expression of synaptic-related proteins and effectively alleviated the synaptic damage induced by depression (Fig. 7). For clarity, we have encapsulated our findings regarding the signaling pathway in a detailed diagram (Fig. 8). However, it is crucial to acknowledge that ATX supplementation could, in some contexts, lead to neurological harm (Wang et al., 2018; Hoelzinger et al., 2008; Kishi et al., 2006). Consequently, it is imperative to discern the appropriate circumstances under which ATX should be administered.

This study acknowledges certain limitations that merit consideration. First, due to the prolonged modeling duration of CUMS, we cannot feasibly sustain the peripheral supplementation of LPA over an extended period while ensuring its efficacious penetration through the BBB. Consequently, our ability to observe the impact of LPA supplementation on depressive-like behaviors is constrained. Second, the LPA receptor inhibitor Ki16425 used in this study inhibits both LPA1 and LPA3 receptors. Due to indications in the literature, it is plausible that LPA3 may not be present in the hippocampus (Suckau et al., 2019), and we infer that the function of LPA may be mediated through the LPA1 receptor, although we cannot completely exclude LPA3's potential role. Thirdly, we chose ELISA as our primary technique for LPA detection instead of mass spectrometry. This decision limits our ability to achieve a more detailed categorization of LPA species. Finally, we have not yet substantiated, at the murine level, the behavioral effects of the drugs LPA, Ki16425, and SCH772984 on mice in the depression model.

In conclusion, the present findings indicate that the ATX-LPA pathway may influence depression-like behaviors by modulating synaptic plasticity in the brains of CUMS-exposed mice. These insights enhance our understanding of depression's etiology and progression concerning lipid metabolism and suggest potential therapeutic approaches for depression.

## Funding

This work was supported by grants from the National Natural Science Foundation of China (grant number: U21A20364) and the Wuhan Health and Family Planning Commission research program funding project (grant number: WX21Q32). This work has not received funding/assistance from any commercial organizations. The funding sources had no roles in the design of this study and will not have any roles during the execution, analyses, interpretation of the data, or decision to submit results.

## CRediT authorship contribution statement

**Chao Wang:** Writing – original draft, Investigation. **Ningyuan Li:** Writing – original draft, Investigation. **Yuqi Feng:** Investigation. **Siqi Sun:** Investigation. **Jingtong Rong:** Investigation. **Xin-hui Xie:** Data curation. **Shuxian Xu:** Writing – review & editing. **Zhongchun Liu:** Writing – review & editing, Project administration.

## Declaration of competing interest

The authors declare that there is no conflict of interest in this work.

## Data availability

Data will be made available on request.

## Appendix A. Supplementary data

Supplementary data to this article can be found online at <https://doi.org/10.1016/j.ynstr.2024.100632>.

## References

- Fujita, R., Ma, Y., Ueda, H., 2008. Lysophosphatidic acid-induced membrane ruffling and brain-derived neurotrophic factor gene expression are mediated by ATP release in primary microglia. *J. Neurochem.* 107 (1), 152–160.
- García-Morales, V., et al., 2015. Membrane-derived phospholipids control synaptic neurotransmission and plasticity. *PLoS Biol.* 13 (5), e1002153.
- Gaynes, B., 2016. Assessing the risk factors for difficult-to-treat depression and treatment-resistant depression. *J. Clin. Psychiatry* 77 (Suppl. 1), 4–8.
- Guo, G., et al., 2020. Testosterone modulates structural synaptic plasticity of primary cultured hippocampal neurons through ERK - CREB signalling pathways. *Mol. Cell. Endocrinol.* 503, 110671.
- Herr, D.R., et al., 2020. Pleotropic roles of autotaxin in the nervous system present Opportunities for the development of Novel therapeutics for neurological diseases. *Mol. Neurobiol.* 57 (1), 372–392.
- Hoelzinger, D.B., et al., 2008. Autotaxin: a secreted autocrine/paracrine factor that promotes glioma invasion. *J. Neuro Oncol.* 86 (3), 297–309.
- Itagaki, K., et al., 2019. Reduced serum and cerebrospinal fluid levels of autotaxin in major depressive disorder. *Int. J. Neuropsychopharmacol.* 22 (4), 261–269.
- Jiang, H., et al., 2021. Tiliainin ameliorates Cognitive dysfunction and neuronal damage in rats with vascular dementia via p-CaMKII/ERK/CREB and ox-CaMKII-dependent MAPK/NF- $\kappa$ B pathways. *Oxid. Med. Cell. Longev.* 2021, 6673967.
- Kim, E.Y., et al., 2018. Serum lipidomic analysis for the discovery of biomarkers for major depressive disorder in drug-free patients. *Psychiatr. Res.* 265, 174–182.
- Kishi, Y., et al., 2006. Autotaxin is overexpressed in glioblastoma multiforme and contributes to cell motility of glioblastoma by converting lysophosphatidylcholine to lysophosphatidic acid. *J. Biol. Chem.* 281 (25), 17492–17500.
- Li, Y., et al., 2019. Antidepressant-like action of single facial injection of botulinum neurotoxin A is associated with augmented 5-HT levels and BDNF/ERK/CREB pathways in mouse brain. *Neurosci. Bull.* 35 (4), 661–672.
- Li, H., et al., 2021. Rifaximin-mediated gut microbiota regulation modulates the function of microglia and protects against CUMS-induced depression-like behaviors in adolescent rat. *J. Neuroinflammation* 18 (1), 254.
- Magkrioti, C., et al., 2019. Autotaxin and chronic inflammatory diseases. *J. Autoimmun.* 104, 102327.
- Omori, W., et al., 2021. Reduced cerebrospinal fluid levels of lysophosphatidic acid docosahexaenoic acid in patients with major depressive disorder and schizophrenia. *Int. J. Neuropsychopharmacol.* 24 (12), 948–955.
- Peñalver, A., et al., 2017. Glutaminase and MMP-9 downregulation in cortex and Hippocampus of LPA(1) receptor null mice correlate with altered dendritic spine plasticity. *Front. Mol. Neurosci.* 10, 278.
- Plastira, I., et al., 2020. MAPK signaling determines lysophosphatidic acid (LPA)-induced inflammation in microglia. *J. Neuroinflammation* 17 (1), 127.
- Robinson, R., 2015. One lipid, two synaptic plasticity pathways. *PLoS Biol.* 13 (5), e1002154.
- Roza, C., et al., 2019. Lysophosphatidic acid and glutamatergic transmission. *Front. Mol. Neurosci.* 12, 138.
- Sánchez-Marín, L., et al., 2018. Systemic blockade of LPA(1/3) lysophosphatidic acid receptors by ki16425 modulates the effects of ethanol on the brain and behavior. *Neuropharmacology* 133, 189–201.
- Sapkota, A., et al., 2020. Lysophosphatidic acid receptor 5 plays a pathogenic role in brain damage after focal cerebral ischemia by modulating neuroinflammatory responses. *Cells* 9 (6).
- Savaskan, N.E., et al., 2007. Autotaxin (NPP-2) in the brain: cell type-specific expression and regulation during development and after neurotrauma. *Cell. Mol. Life Sci.* 64 (2), 230–243.
- Shupliakov, O., Haucke, V., Pechstein, A., 2011. How synapsin I may cluster synaptic vesicles. *Semin. Cell Dev. Biol.* 22 (4), 393–399.
- Suckau, O., et al., 2019. LPA(1), LPA(2), LPA(4), and LPA(6) receptor expression during mouse brain development. *Dev. Dynam.* 248 (5), 375–395.
- Thiel, G., Synapsin, I., 1993. Synapsin II, and synaptophysin: marker proteins of synaptic vesicles. *Brain Pathol.* 3 (1), 87–95.
- Vogt, J., et al., 2016. Molecular cause and functional impact of altered synaptic lipid signaling due to a prg-1 gene SNP. *EMBO Mol. Med.* 8 (1), 25–38.
- Walker, T.L., et al., 2016. Lysophosphatidic acid receptor is a functional marker of adult hippocampal precursor cells. *Stem Cell Rep.* 6 (4), 552–565.
- Wang, C., et al., 2018. Lysophosphatidic acid induces neuronal cell death via activation of asparagine endopeptidase in cerebral ischemia-reperfusion injury. *Exp. Neurol.* 306, 1–9.
- Xue, W., et al., 2009. Polygalasaponin XXXII from *Polygala tenuifolia* root improves hippocampal-dependent learning and memory. *Acta Pharmacol. Sin.* 30 (9), 1211–1219.
- Yan, L., et al., 2020. Antidepressant-like effects and cognitive enhancement of coadministration of chailu shugan san and fluoxetine: dependent on the BDNF-ERK-CREB signaling pathway in the Hippocampus and frontal cortex. *BioMed Res. Int.* 2020, 2794263.
- Yao, W., et al., 2022. Microglial ERK-NRBP1-CREB-BDNF signaling in sustained antidepressant actions of (R)-ketamine. *Mol. Psychiatry.* 27 (3), 1618–1629.
- Yung, Y.C., et al., 2015. Lysophosphatidic Acid signaling in the nervous system. *Neuron* 85 (4), 669–682.
- Zhang, B., et al., 2020. DL0410 attenuates oxidative stress and neuroinflammation via BDNF/TrkB/ERK/CREB and Nrf2/HO-1 activation. *Int. Immunopharm.* 86, 106729.